Iran J Ped Hematol Oncol. 2026, Vol. 16, No. 2, 812-825

Original Article

Synthesis of Dihydropyrano[3,2-c]chromenes in the Presence of Effective Acid–Base Nano Catalyst (3-Aminopyridine/Go) and Evaluation of Their Toxicity against Cancer Cells

Hamideh Emtiazi PhD[1,2*], Leila Amiri-Zirtol PhD[3], Hadi Zare Zardini PhD[2,4*], Amir Abbas Mohammadi Hamaneh PhD[5], Soghra Khabnadideh PhD[3], Bebe Zahra Modaresi PhD[6]

[1]Faculty of Pharmacy, Shahid Sadoughi University of Medical Sciences, Yazd, Iran
[2]Hematology and Oncology Research Center, Shahid Sadoughi University of Medical Sciences, Yazd, Iran
[3]Pharmaceutical Sciences Research Center, Shiraz University of Medical Sciences, Shiraz, Iran
[4]Department of Biomedical Engineering, Meybod University, Meybod, Iran
[5]Department of pharmacology, School of medicine, Tehran university of medical sciences, Tehran, Iran
[6]Chemical Engineering (Biotecnology), Faculty of Engineering, University of Tehran, Iran
*Corresponding Authors: Dr. Hamideh Emtiazi, Faculty of Pharmacy, Shahid Sadoughi University of Medical Sciences, Yazd, Iran. Email: Hamideh.emtiazi@yahoo.com. ORCID ID: 0000-0001-7883-5145; Dr. Hadi Zare-Zardini, Department of Biomedical Engineering, Meybod University, Meybod, Iran. Email: hzare@meybod.ac.ir. ORCID ID: 0000-0002-1501-2560

Received: April 16, 2025;
Accepted: October 08, 2025

[Downloaded from ijpho.ssu.ac.ir on 2026-11-24]

[DOI: 10.18502/ijpho.v16i2.21344]

Abstract

Background: Dihydropyrano[3,2-c]chromenes are oxygen-containing heterocycles with reported anticancer potential, yet green and efficient synthetic methods remain limited. Conventional catalysts often involve harsh conditions or low reusability. This study aimed to develop a sustainable, high-yield synthesis of chromenes via a novel acid–based nanocatalyst (GO/3-aminopyridine), and to evaluate the cytotoxicity of selected derivatives against cancer and normal cells.

Materials and Methods: In this in vitro experimental study, we performed a one-pot, three-component reaction of 4-hydroxycoumarin, malononitrile or ethyl cyanoacetate, and aromatic aldehydes in the presence of 3-aminopyridine-functionalized graphene oxide (GO/3-APy) under mild conditions (EtOH/H_2O, 50 °C). The structure of the catalyst and products were confirmed via FT-IR, NMR, XRD, FE-SEM, and EDS. MTT assay was used to determine IC_{50} values for selected compounds against Ovcar3, T47D, CA46, and HFF cell lines. Doxorubicin served as a positive control. Statistical analyses were done by SPSS (Version 22.0). ANOVA test was performed to identify significant differences in IC_{50} values across all tested compounds and doxorubicin. p-value < 0.05 was considered significant.

Results: Compound 4b exhibited potent cytotoxicity against Ovcar3 (IC_{50} = 14.67 ± 1.15 µg/mL), T47D (26.85 ± 2.10 µg/mL), and CA46 (27.17 ± 1.55 µg/mL) cells, significantly surpassing doxorubicin against CA46 (46.07 ± 2.80 µg/mL; $p < 0.05$). Compound 4d showed comparable activity (IC_{50} = 17.99 ± 1.42, 29.50 ± 1.85, and 56.62 ± 2.90 µg/mL, respectively) with high selectivity for cancer cells over normal HFF (IC_{50} = 239.25 ± 5.50 µg/mL; selectivity index ~13). Compounds 4e, 4g, and 4h demonstrated moderate cytotoxicity (IC_{50} = 33.50–141.52 µg/mL), while doxorubicin displayed non-selective toxicity toward normal cells (IC_{50} = 50.45 ± 2.90 µg/mL vs. 239.25 µg/mL for 4d).

Conclusion: The results of our research showed that dihydropyrano[3,2-c]chromene derivatives showed anticancer effects that depended on the type of substitution present on the ring in their structure.

Keywords: 3-Aminopyridine, Cancer, Doxorubicin, Graphene oxide

This article is distributed under the terms of the Creative Commons Attribution-NonCommercial 4.0 International License.

Introduction

The chromene nucleus represents a key structural motif in numerous biologically active compounds. Among its derivatives, dihydropyrano[3,2-c]chromenes have received considerable attention due to their wide range of therapeutic properties, such as antioxidant, anticoagulant, antitumor, antifungal, and antibacterial activities (1–6). Specifically, these compounds have demonstrated anticancer effects through mechanisms including enzyme inhibition, induction of apoptosis, and selective cytotoxicity toward resistant cancer cells (7).

Numerous catalytic strategies have been employed for the synthesis of dihydropyrano[3,2-c]chromenes, using various catalysts such as $H_6P_2W_{18}O_{62}\cdot 18H_2O$, hexamethylenetetramine, CuO nanoparticles, thiourea dioxide, sodium bromide, dimethylaminopyridine-functionalized ionic liquids, graphene oxide–based nanocatalysts, nano-SiO_2, MgO, o-benzenedisulfonimide, mefenamic acid, and other organic–inorganic hybrid systems (8–21). Despite these developments, many reported methods still suffer from key limitations, including the use of toxic reagents, elevated temperatures, long reaction times, low yields, and difficulty in catalyst recovery or reuse.

As a result, continued development of more efficient, eco-friendly, and reusable catalytic systems remains a priority, especially in the context of green chemistry. Heterogeneous catalysts are of particular interest due to their ease of separation, reusability, and reduced environmental impact. Among various supports, graphene oxide (GO) is one of the most promising due to its high surface area, excellent thermal and chemical stability, and abundance of functional groups such as hydroxyl, epoxy, carbonyl, and carboxyl moieties, which allow for tunable catalytic activity (22, 23). GO can also be readily functionalized with nitrogen-containing organic molecules to further enhance its performance.

3-Aminopyridine, a basic heterocyclic compound, can be covalently anchored onto the GO surface to produce a bifunctional nanocatalyst with both acid and base properties. The carboxylic acid groups of GO provide acidity, while the basic nitrogen centers of 3-aminopyridine facilitate deprotonation and nucleophilic activation (24,25). This dual acid–base functionality is especially advantageous in multi-component reactions such as the synthesis of dihydropyrano[3,2-c]chromenes, which require both electrophilic and nucleophilic activation. The acidic sites promote activation of aldehyde carbonyl groups, while the basic sites assist in malononitrile deprotonation, thus enabling Knoevenagel condensation and Michael addition to proceed efficiently under mild conditions.

The covalent bonding of 3-aminopyridine on GO increases the interlayer spacing, enhances accessibility to catalytic sites, and prevents leaching, as evidenced by XRD and other characterization techniques. The resulting nanocatalyst demonstrates high efficiency at 50 °C in ethanol/water media, achieving high yields in short times under green conditions and enabling facile separation and reuse.

This study focuses on the design and application of GO/3-aminopyridine as a dual-functionality nanocatalyst for the green synthesis of dihydropyrano[3,2-c]chromenes. The synthesized compounds were further evaluated for their in vitro cytotoxicity against several cancer cell lines (OVCAR3, T47D, CA46) and a normal fibroblast line (HFF) to identify potent and selective anticancer candidates.

Material and Methods

All reagents were purchased from Merck and Aldrich and used without further purification. Products were characterized by IR, 1H-NMR, and 13C-NMR spectra. IR spectra were recorded on a Bruker Equinox 55 spectrometer. 1H-NMR, and 13C-NMR spectra were obtained using Bruker Avance 400 and 100 MHz spectrometers (DRX), respectively. Melting points were recorded using a Buchi B-540 B.V.CHI device. FE-SEM (MIRA3 TESCAN XMU) was used to assess and compare the surfaces of the composite and GO. SAMX MIRA II was employed for EDS analysis. Composite crystallographic characterization was performed with X'Pert PRO MPD P decomposition, using Ni-filtered Cu-Kα radiation in the diffraction angle range of 5–80°.

[Downloaded from ijpho.ssu.ac.ir on 2026-11-24]

[DOI: 10.18502/ijpho.v16i2.21344]

This article is distributed under the terms of the Creative Commons Attribution-NonCommercial 4.0 International License.

Synthesis of nano-GO/3-aminopyridine

The GO/3-aminopyridine nanocatalyst was synthesized in two steps under mild conditions (Figure 1). In the first step, graphene oxide was produced following the Hummers method as described in the referenced publications, which involves oxidizing graphite with a mixture of concentrated sulphuric acid, sodium nitrate, and potassium permanganate (26). Then, 3-aminopyridine was stabilized on graphene oxide sheets in ethanol solvent at reflux temperature.

General method for the synthesis of dihydropyrano[3,2-c]chromenes

For the synthesis of dihydropyrano[3,2-c]chromenes, malononitrile, 4-hydroxycoumarin, and various aldehydes were reacted in the presence of nano-3-aminopyridine/GO at 50 °C using EtOH/H2O as the solvent, producing dihydropyranochromene products (a–h) (Figure 1). The progress of the reaction was monitored by thin layer chromatography. Crystallization in ethanol was used to purify the resulting products.

Spectroscopic data for dihydropyrano[3,2-c]chromenes

2-Amino-4-(phenyl)-3-carbonitrile-4,5-dihydro-pyrano[2,3-c]chromene-5-one (a)

Yield: 90%, White solid, m.p. 255-257°C .

FT- IR: νmax (ATR, neat) = 3324 (NH stretch), 3305 (NH stretch), 3186 (NH stretch), 2207 (CN stretch), 1708 (CO stretch), 1619, 1587, 1437, 1380, 1269 cm-1

1H NMR (500 MHz, DMSO-d6): δ = 4.42 (s, 1H), 7.19-7.24 (m, 5H), 7.27-7.47 (m, 4H), 7.67 (t, J=8.0 Hz, 1H), 8.87 (d, J=8.0 Hz, 1H).

13C NMR (125 MHz, DMSO-d6) δ (ppm): 57.60, 104.00, 112.96, 116.50, 119.26, 122.36, 124.73, 124.80, 127.14, 127.65, 128.50, 133.00, 143.06, 152.10, 153.42, 157.96, 159.66.

2-Amino-4-(4-bromophenyl)-3-carbonitrile-4,5-dihydro-pyrano[2,3-c]chromene-5-one (b)

Yield: 92%, White solid, m.p. 274-275 °C.

FT- IR: νmax (ATR, neat) = 3369 (NH stretch), 3323 (NH stretch), 3201 (NH stretch), 2202 (CN stretch), 1703 (CO stretch), 1669, 1606, 1381, 1305, 1261 cm-1

1H NMR (500 MHz, DMSO-d6): δ = 4.46 (s, 1H), 7.25 (d, J=5.0 Hz, 2H), 7.41-7.55 (m, 6H), 7.75 (t, J=8 Hz, 1H), 7.65-7.93 (t, J=8.0 Hz, 1H).

2-Amino-4-(2-bromophenyl)-3-carbonitrile-4,5-dihydro-pyrano[2,3-c]chromene-5-one (c)

Yield: 90%, White solid, m.p. 247-249°C.

FT- IR: νmax (ATR, neat) = 3403 (NH stretch), 3318 (NH stretch), 3196 (NH stretch), 2202 (CN stretch), 1701 (CO stretch), 1670, 1529, 1381, 1346, 1262 cm-1

1H NMR (400 MHz, DMSO-d6): δ = 4.42 (s, 1H), 7.45 (d, J=8.0 Hz, 1H), 7.50 (t, J=8.0 Hz, 1H), 7.56 (S, 2H), 7.63 (t, J=8.0 Hz, 1H), 7.72 (t, J=8.0 Hz, 1H), 7.81 (d, J=8.0 Hz, 1H), 7.91 (d, J=8.0 Hz, 1H), 8.13 (m, 2 H).

2-Amino-4-(4-methoxyphenyl)-3-carbonitrile-4,5-dihydro-pyrano[2,3-c]chromene-5-one (d)

Yield: 82%, White solid, m.p. 246-248 °C

FT- IR: νmax (ATR, neat) = 3368 (NH stretch), 3179 (NH stretch), 2202 (CN stretch), 1703 (CO stretch),1672, 1640, 1612, 1376, 1171, 1112 cm-1

1H NMR (500 MHz, DMSO-d6): δ = 3.35 (S, 3H), 4.41 (s, 1H), 6.75 (dd, J=8.0 Hz, 1H), 6.85-6.90 (m, 3H), 7.35 (s, 2H), 7.45-7.53 (m, 2H), 7.70 (t, 1H), 7.89 (dd, J=8 Hz, J=4 Hz 1H).

13C NMR (125 MHz, DMSO-d6) δ (ppm): 55.49, 58.11, 66.34, 78.97, 101.95, 104.11, 106.59, 112.22, 113.05, 116.66, 119.34, 119.67, 124.69, 135.84, 147.93, 148.50, 152.11, 153.18, 157.92,159.60.

2-Amino-4-(4-fluorophenyl)-3-carbonitrile-4,5-dihydro-pyrano[2,3-c]chromene-5-one (e)

Yield: 94%, White solid, m.p. 260-262°C .

FT- IR: νmax (ATR, neat) = 3374 (NH stretch), 3292 (NH stretch), 3190 (NH stretch), 2194 (CN stretch), 1713 (CO stretch), 1674, 1639, 1505, 1376, 1059 cm-1

1H NMR (500 MHz, DMSO-d6): δ = 4.32 (S, J=8.0 Hz, 1H), 7.19 (t, J=8.0 Hz, 2H), 7.37 (m, 2H), 7.50-7.60 (m, 4H), 7.75-7.82 (t, J=8.0 Hz, 1H), 7.96 (d, J=8.0 Hz, 1H).

2-Amino-4-(2-fluorophenyl)-3-carbonitrile-4,5-dihydro-pyrano[2,3-c]chromene-5-one (f)

Yield: 89%, White solid, m.p. 250-252°C .

FT- IR: νmax (ATR, neat) = 3358 (NH stretch), 3190 (NH stretch), 2202 (CN stretch), 1713 (CO stretch), 1670, 1603, 1494, 1454, 1390, 1312, 1279, 1179 cm-1

1H NMR (500 MHz, DMSO-d6): δ = 5.25 (S, 1H), 7.44-7.54 (m, 6H), 7.65 (t, J=8.0 Hz, 1H), 7.72

[Downloaded from ijpho.ssu.ac.ir on 2026-11-24]

[DOI: 10.18502/ijpho.v16i2.21344]

This article is distributed under the terms of the Creative Commons Attribution-NonCommercial 4.0 International License.

(t, J=8.0 Hz, 1H), 7.90 (d, J=8.0 Hz, 2H).

2-Amino-4-(3-pyridil)-3-carbonitrile-4,5-dihydro-pyrano[2,3-c]chromene-5-one (g)

Yield: 87%, White solid, m.p. 251-253°C.

FT- IR: νmax (ATR, neat) = 3376 (NH stretch), 3292 (NH stretch), 3190 (NH stretch), 2194 (CN stretch), 1713 (CO stretch), 1674, 1639, 1460, 1377, 1213 cm-1.

1H NMR (400 MHz, DMSO-d6): δ = 4.56 (s, 1H), 7.35 (t, J=7.2 Hz, 1H), 7.46-7.53 (m, 4H), 7.71-7.75 (m, 2H), 7.90 (d, J=6.8 Hz, 1H), 8.46 (d, J=4.0 Hz, 1H), 8.55 (s, 1H).

13C NMR (125 MHz, DMSO-d6) δ (ppm): 34.65, 56.96, 102.92, 112.96, 116.57, 119.03, 122.54, 123.79, 124.66, 133.02, 135.45, 138.75, 143.23, 149.03, 152.21, 153.79, 158.02, 159.56.

2-Amino-4-(4-pyridil)-3-carboethoxy-4,5-dihydro-pyrano[2,3-c]chromene-5-one (h)

Yield: 89%, White solid, m.p. 260-262 °C.

FT- IR: νmax (ATR, neat) = 3358 (NH stretch), 3232 (NH stretch), 1715 (CO stretch), 1688, 1658, 1549, 1373, 1278, 1198 cm-1

1H NMR (400 MHz, DMSO-d6): δ =1.10 (t, J=7.2 Hz, 3H), 4.00 (q, J=6.8 Hz, 2H), 4.74 (s, 1H), 7.42 (d, J=6.2 Hz, 2H), 7.48 (d, J=8.2 Hz, 1H), 7.51 (t, J=8.0 Hz, 1H), 7.72 (t, J=8.0 Hz, 1H), 7.76 (d, J=8.0 Hz, 1H), 8.00 (br s, 2H), 8.51 (d, J=6.2 Hz, 2H).

13C NMR (125 MHz, DMSO-d6) δ (ppm): 14.11, 35.34, 59.17, 62.13, 104.89, 112.98, 116.58, 122.62, 123.9, 124.15, 130.78, 133.02, 145.18, 147.66, 152.2, 155.59, 158.57, 159.86, 167.14.

Anal. Calcd for C19H16N2O5: C, 64.77; H, 4.54; N, 7.95; O, 22.72. Found: C, 64.50; H, 4.42; N, 7.86; O, 22.80.

Catalyst recycling and hot-filtration

Catalyst recycling protocol

The reusability of GO/3-aminopyridine (0.03 g) was evaluated in the model three-component synthesis of 4a (4-hydroxycoumarin 1.0 mmol, benzaldehyde 1.0 mmol, malononitrile 1.0 mmol) in EtOH/H2O (1:1, 5 mL) at 50 °C. After the reaction was complete, the solid catalyst was separated from the reaction mixture, washed with ethanol (3 × 10 mL), dried at 60 °C, then weighed and reused under the same conditions. Isolated yields, reaction time, and mass of the recovered catalyst were recorded for five consecutive cycles.

Hot-filtration (leaching) test

The model reaction was allowed to reach approximately 50% conversion (~6 min), after which the hot mixture was quickly filtered to remove the solid catalyst. The resulting filtrate was stirred at 50 °C for a further 12 min; no significant progress was observed (Δconversion ≤ 2%), indicating minimal leaching of active species.

Assessment of cytotoxicity

Cell culture

Breast cancer (T47d), Human Burkitt's Lymphoma (CA46), Ovarian cancer (OVCAR3), and human foreskin fibroblast (HFF) cell lines were obtained from the Pasteur Institute of Iran. The cells were cultured in DMEM (Dulbecco's Modified Eagle Medium) supplemented with 10% FBS (fetal bovine serum) and 1% penicillin-streptomycin in an incubator under standard conditions (5% CO2, 37 °C, and 95% humidity). After three passages, subsequent procedures and determination of the number of viable cells were performed.

MTT assay

To measure the toxic effects of dihydropyrano[3,2-c]chromenes, the MTT [3-(4,5-dimethyl-2-thiazolyl)-2,5-diphenyl-2H-tetrazolium bromide] assay was used. MTT powder is a water-soluble thiazolyltetrazolium bromide salt that is converted into an insoluble formazan compound upon reduction. In this assay, viable cells exposed to the MTT solution produce a purple precipitate. After dissolving this precipitate in a suitable solvent, the optical density of the samples is measured. The absorbance of this compound, after dissolution in DMSO, can be measured at 570–590 nm.

The procedure is as follows: after passaging and counting the cells using a haemocytometer, 1 × 10^4 cells were added to each well of a 96-well plate and incubated for 24 hours with serum-containing culture medium in a CO2 incubator to allow the cells to adhere to the bottom of the wells. The wells were then washed with PBS buffer and treated with 100 microlitres of fresh medium along with 20 microlitres of the test compounds at concentrations of 12.5, 25, 50, 75, and 100 µg/ml. Each treatment was performed in triplicate. The plates were then incubated in a CO2 environment

[Downloaded from ijpho.ssu.ac.ir on 2026-11-24]

[DOI: 10.18502/ijpho.v16i2.21344]

This article is distributed under the terms of the Creative Commons Attribution-NonCommercial 4.0 International License.

for 24, 48, and 72 hours at 37°C. After these incubation periods, the supernatant from each well was removed, the wells were washed with buffer, and the cells were washed with 100 microlitres of fresh medium without serum. Then, 10 microlitres of MTT solution (2.5 mg/mL in phosphate-buffered saline) was added to each well and incubated for 2 hours. After this period, the supernatant from the wells was removed and 150–200 µl of DMSO (dimethyl sulfoxide) was added to each well for cell lysis. The optical density (OD) of each well was then measured at a wavelength between 570 and 590 nm using an ELISA reader, and cell viability was calculated using the following formula (27):

Viability percent = OD Control / OD Test × 100

A concentration of the compounds that reduced cell viability by half was considered the IC50 (half maximal inhibitory concentration). Control groups included those treated with 0.1% DMSO (negative control) and 10 µM doxorubicin (positive control).

Statistical analysis

This study constitutes an in vitro experimental investigation. The IC_{50} values for all tested compounds were determined via the MTT assay. Each experiment was performed in technical triplicate and repeated across three independent biological replicates (n = 3). Thus, each reported IC_{50} value represents the mean ± standard deviation (SD) derived from nine individual measurements (3 replicates × 3 independent experiments). Prior to conducting parametric statistical analyses, the normality of data distribution for all IC_{50} datasets was rigorously verified using the Shapiro-Wilk test (significance level $\alpha = 0.05$). All groups exhibited a normal distribution ($p > 0.05$), thereby validating the application of parametric statistical methods. The selection of three independent biological replicates (n = 3) adheres to internationally recognized standards for in vitro cytotoxicity testing and ensures adequate statistical power (>80%) to detect clinically meaningful differences. For each cell line (Ovcar3, T47D, CA46, and HFF), one-way analysis of variance (ANOVA) was performed to identify significant differences in IC_{50} values across all tested compounds and doxorubicin (positive control). All statistical analyses were executed using IBM SPSS Statistics for Windows, Version 22.0 (IBM Corp., Armonk, NY, USA). A p-value < 0.05 was considered statistically significant.

Results

Initially, we synthesized the nanocatalyst through a two-step process illustrated in Figure 1.

In the next stage, to determine the optimal reaction conditions for the synthesis of chromenes, a model reaction involving benzaldehyde, 4-hydroxycoumarin, and malononitrile was conducted under various temperature, catalytic, and solvent conditions, and the best conditions were selected (Figure 2 and Table I). According to Table I, row 9, the optimal conditions for this reaction are the use of water and ethanol (1:1) as the solvent at a temperature of 50 ºC, with 0.03 grams of the desired catalyst.

After optimizing the reaction conditions using the model reaction, the scope and generality of this method were explored. A diverse library of dihydropyrano[3,2-c]chromenes was synthesized via the three-component reaction of 4-hydroxycoumarin, various aromatic aldehydes, and malononitrile or ethyl cyanoacetate as shown in Figure 3. The results, including reaction times and isolated yields, are summarized in Table II.

XRD patterns of the GO/3-aminopyridine composite are shown in Figure 3. Functionalized graphene oxide exhibits a characteristic peak in the region of $2\theta = 10°$. The interlayer distance was calculated using the Bragg equation: $n\lambda = 2d \sin\theta$. The distance between the functionalized graphene oxide layers is 0.884 nm, which is greater than that of GO, where the interlayer distance is 0.85 nm (25). This increase in distance is attributed to the presence of organic compounds between the graphene oxide layers, which in turn caused the shift of the XRD peak (Figure 4).

The FT-IR spectra of graphene oxide (GO), 3-aminopyridine, and the nano-GO/3-aminopyridine composite are presented in Figure 5. Comparison of the spectra of GO and GO/3-aminopyridine shows changes in the absorption bands of GO before and after functionalisation. In the FT-IR spectrum of GO, a peak at 3398 cm−1 corresponds to the stretching vibrations of the OH groups present on the GO sheets and the

[Downloaded from ijpho.ssu.ac.ir on 2026-11-24]

[DOI: 10.18502/ijpho.v16i2.21344]

This article is distributed under the terms of the Creative Commons Attribution-NonCommercial 4.0 International License.

carboxylic acid groups within the GO structure. Peaks at 1719 cm−1 and 1618 cm−1 are associated with the stretching vibrations of the C=O and C=C groups, while the peak around 1041 cm−1 is attributed to C–O vibrations (25).

The spectrum of 3-aminopyridine also exhibits notable peaks. The peaks at 3373 cm−1 and 3316 cm−1 are due to NH2 stretching vibrations. The stretching vibration of the NH group is indicated by the absorption at 3342 cm−1, while the peak at 3199 cm−1.

The FT-IR spectrum of the functionalized GO shows significant alterations. The appearance and disappearance of various peaks indicate the attachment of the organic molecule to the surface of GO.

EDS (Energy-dispersive X-ray spectroscopy) can be used to identify the elements present in a sample.

The EDS analysis of the composite shown in Figure 6 indicates that the catalyst structure contains nitrogen (N) in addition to oxygen (O) and carbon (C), confirming the incorporation of 3-aminopyridine into the composite. According to this analysis, the percentages of C, N, and O in the catalyst were determined to be 52.53%, 12.05%, and 35.42%, respectively.

SEM analysis is used to examine the morphology of the synthesized composite. The morphology of GO/3-aminopyridine is shown in Figure 7 (a–c). The images illustrate changes in surface morphology at three magnifications: 5 µm, 1 µm, and 100 nm. In all three images, changes in the composite surface are clearly visible. In Figure a, the layered nature of the composite is evident. In image b, the layers display fine grains on their surface, which are more apparent in image c. This structural change indicates the formation of a composite and a modification of the graphene oxide surface.

Under optimized conditions, GO/3-aminopyridine was reused for five consecutive runs in the model synthesis of 4a, with only a slight decrease in performance (Table III and Figure 8). The isolated yields remained high, from 90% (cycle 1) to 87% (cycle 5), while the reaction time increased slightly. The recovered catalyst mass decreased only marginally over five cycles, indicating good mechanical stability and practical reusability under mild EtOH/H2O conditions. A hot-filtration test carried out at approximately 50% conversion showed no further progress in the filtrate over 12 minutes (Δconversion ≤ 2%), supporting a truly heterogeneous process with negligible leaching.

The effects of selected synthesized compounds on ovarian (Ovcar3), breast (T47D), and lymphoma (CA46) cancer cell lines, as well as a normal cell line (HFF), were investigated (Table IV and Figure 9).

Table I. Optimization of the reaction conditions

Entry	Catalyst	g	Temperature (°C)	Solvent	Time (min)	Yield (%)
1	-	-	50	EtOH	60	40
2	GO	0.04	50	EtOH	60	45
3	GO/3-aminopyridine	0.04	50	EtOH	12	93
4	GO/3-aminopyridine	0.04	50	EtOH /H_2O(1:1)	12	93
5	GO/3-aminopyridine	0.04	50	H2O	30	85
6	GO/3-aminopyridine	0.04	50	Solvent-free	60	75
7	GO/3-aminopyridine	0.04	r.t	EtOH /H_2O(1:1)	34	80
8	GO/3-aminopyridine	0.04	reflux	EtOH / H_2O (1:1)	12	93
9	**GO/3-aminopyridine**	**0.03**	**50**	**EtOH / H_2O (1:1)**	**12**	**93**
10	GO/3-aminopyridine	0.02	50	EtOH / H_2O (1:1)	38	80
11	GO/3-aminopyridine	0.01	50	EtOH / H_2O (1:1)	60	50

GO: Graphen oxide EtOH: Ethanol

[Downloaded from ijpho.ssu.ac.ir on 2026-11-24]

[DOI: 10.18502/ijpho.v16i2.21344]

This article is distributed under the terms of the Creative Commons Attribution-NonCommercial 4.0 International License.

Table II. Synthesis of various dihydropyrano[3,2-c]chromenes under optimized conditions

Entry	RCHO	Z	Yield %	Time (min)	M.P. (°C)
4a	C_6H_5-	CN	90	12	**255-257**[11]
4b	4-(Br)-C_6H_4-	CN	92	10	**274-275**[31]
4c	2-(Br)-C_6H_4-	CN	90	13	**247-249**[11]
4d	4-(OCH_3)-C_6H_4-	CN	82	15	**246-248**[31]
4e	4-(F)-C_6H_4-	CN	94	11	**260-262**[11]
4f	2-(F)-C_6H_4-	CN	89	16	**250-252**[11]
4g	3- C_5H_4N	CN	87	20	**251-253**[31]
4h	4- C_5H_4N	$CO_2C_2H_5$	89	15	**260-262**

M. P. : Melting point, GO: Graphen oxide

Table III. Recycling performance of GO/3-aminopyridine in the model synthesis of 4a under optimized conditions (EtOH/H2O 1:1, 50 °C, 0.03 g catalyst).

Cycle	Time (min)	Isolated yield (%)
1	12	90
2	15	90
3	20	87
4	20	88
5	20	87

Table IV. In vitro cytotoxicity (IC50, µg/mL) of selected dihydropyrano[3,2-c]chromenes against cancer and normal cell lines.

Compound	Ovcar3	T47D	CA46	HFF
4b	14.67 ± 1.15	26.85 ± 2.10	27.17 ± 1.55	58.55 ± 3.20
4d	17.99 ± 1.42	29.50 ± 1.85	56.62 ± 2.90	239.25 ± 5.50
4e	37.05 ± 2.20	33.50 ± 2.05	49.41 ± 1.95	202.40 ± 4.80
4g	69.65 ± 3.10	29.80 ± 1.50	141.52 ± 4.20	178.90 ± 5.10
4h	36.48 ± 2.05	37.89 ± 2.30	35.50 ± 2.15	122.95 ± 3.75
Doxorubicin	15.53 ± 1.25	34.28 ± 2.45	46.07 ± 2.80	50.45 ± 2.90

Data are expressed as Mean ± Standard Deviation (SD) from three independent experiments (n=3).

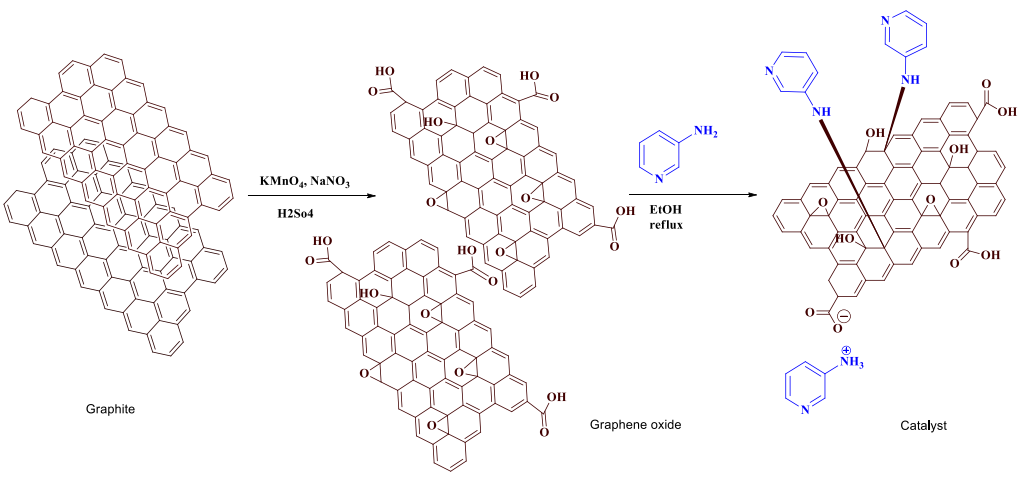


Figure 1. Synthesis of nano-GO/3-aminopyridine

[Downloaded from ijpho.ssu.ac.ir on 2026-11-24]

[DOI: 10.18502/ijpho.v16i2.21344]

This article is distributed under the terms of the Creative Commons Attribution-NonCommercial 4.0 International License.

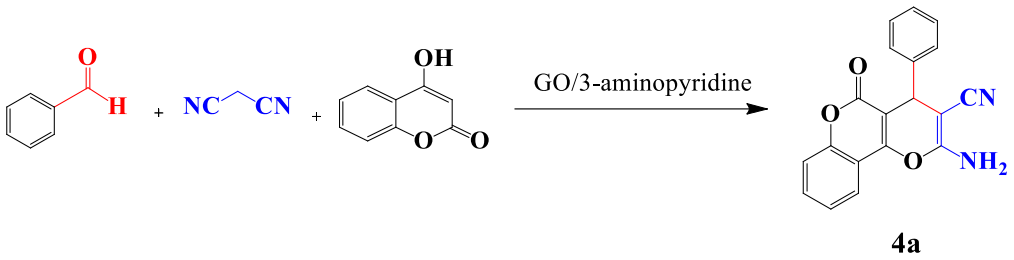


Figure 2. Synthesis of dihydropyrano[3,2-c]chromene derivative

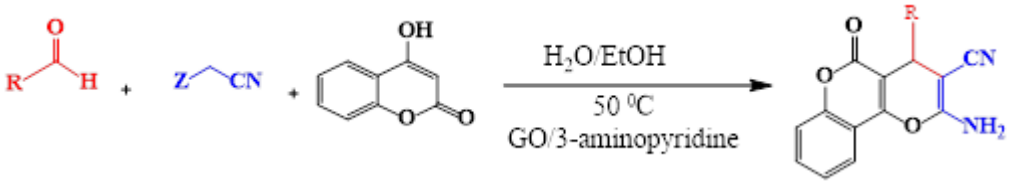


Figure 3. Synthesis of various dihydropyrano[3,2-c]chromene derivatives (4a–h) catalyzed by nano-GO/3-aminopyridine under optimized conditions

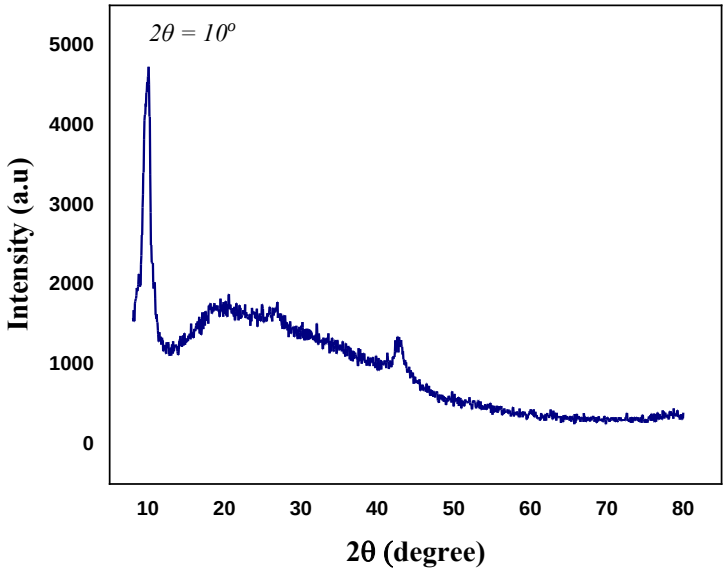


Figure 4. XRD pattern of nano-GO/3-aminopyridine

[Downloaded from ijpho.ssu.ac.ir on 2026-11-24]

[DOI: 10.18502/ijpho.v16i2.21344]

This article is distributed under the terms of the Creative Commons Attribution-NonCommercial 4.0 International License.

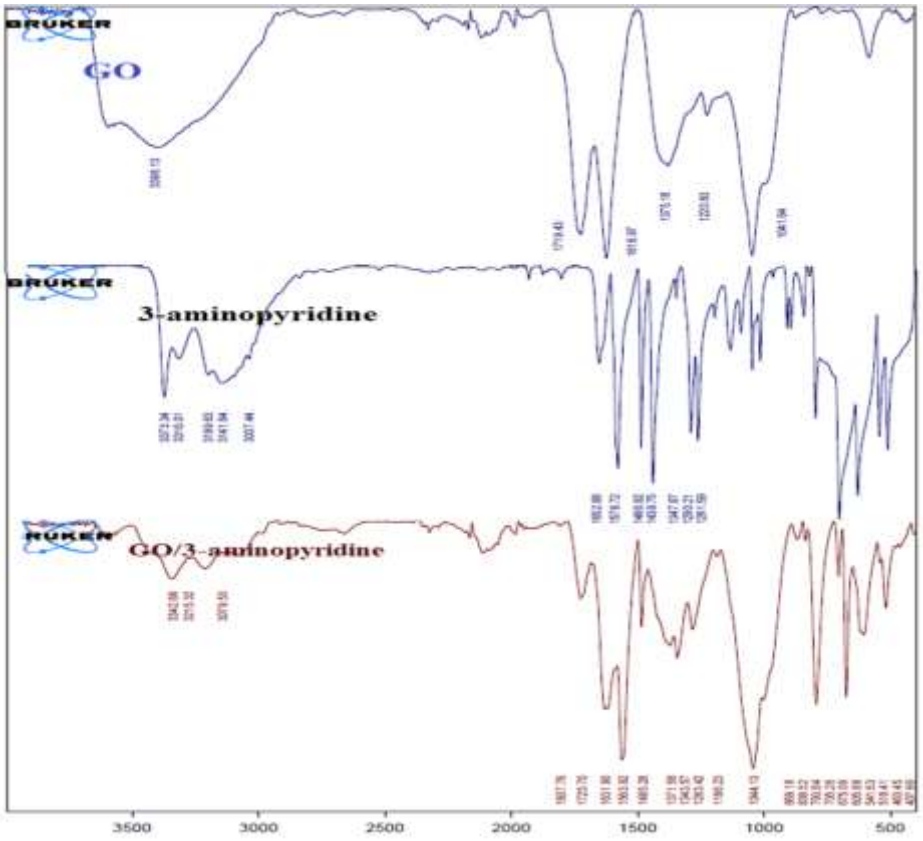


Figure 5. The FT-IR spectra of three compounds, GO, 3-aminopyridine and GO / 3-aminopyridine

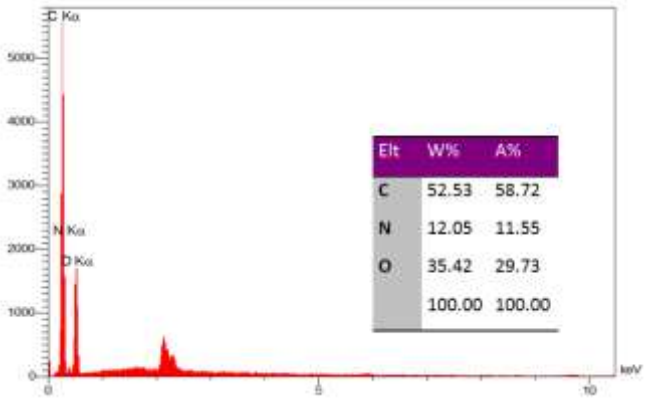


Figure 6. EDS analysis of nano-GO/3-aminopyridine

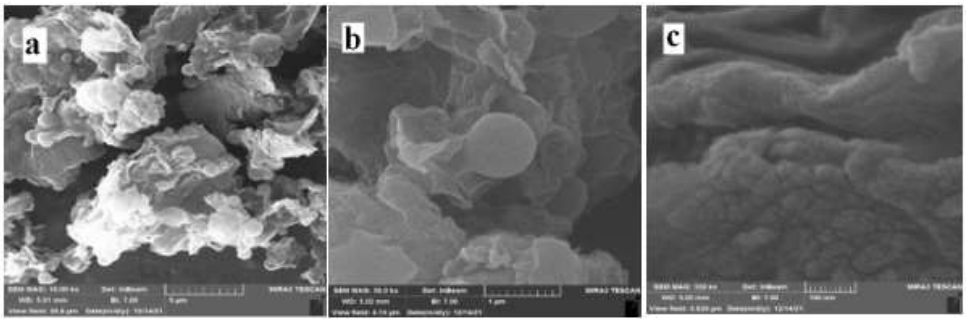


Figure 7. FE-SEM image of nano-GO/3-aminopyridine, a: 5 µm b: 1 µm c: 100 nm

[Downloaded from ijpho.ssu.ac.ir on 2026-11-24]

[DOI: 10.18502/ijpho.v16i2.21344]

This article is distributed under the terms of the Creative Commons Attribution-NonCommercial 4.0 International License.

Discussion

The catalytic efficiency of the nano-GO/3-aminopyridine composite in the synthesis of dihydropyrano[3,2-c]chromenes underscores the significance of heterogeneous dual acid-base systems in modern organic chemistry. The catalytic efficiency of the synthesized GO/3-aminopyridine composite can be better understood in comparison to previously reported systems. For instance, Si-Mg-FA as a catalyst required 60 minutes under reflux conditions in EtOH/H_2O to yield the desired chromene product (28). Similarly, $H_6[P_2W_{18}O_{62}]\cdot 18H_2O$ also achieved product formation in 60 minutes under refluxing EtOH/H_2O (8). Nano ZnO required 120 minutes at 90 °C (29), while the SDS catalyst took 180 minutes in pure water under reflux to afford the products (30). A more recent approach using nano-SiO_2 functionalized with DBN achieved the desired chromenes in 15 minutes under reflux in EtOH/H_2O (31), which although faster, still relied on harsher thermal conditions. Another reported method using ammonium trifluoroacetate (CF_3COONH_4) required up to 180 minutes under similar reflux conditions in EtOH/H_2O medium (32).

By contrast, the GO/3-aminopyridine nanocatalyst in the present study enabled the synthesis of dihydropyrano[3,2-c]chromene derivatives in just 12 minutes at 50 °C using a green EtOH/H_2O solvent system. This notable reduction in reaction time-without the need for reflux-and the ability to operate at a significantly lower temperature highlight the superior performance of the developed catalyst. Furthermore, the reaction achieved a high yield (up to 93%) under these optimized mild conditions, illustrating a more efficient and sustainable strategy compared to traditional methods.

This enhancement in catalytic performance can be attributed to the synergistic acid–base functionality of the GO/3-aminopyridine composite, the increased accessibility of active sites due to the expanded interlayer distance, and the material's robust chemical structure, all of which contribute to faster kinetics and higher conversions under environmentally benign conditions.

The superior performance is due to the unique structural architecture of the catalyst. The high surface area of graphene oxide, decorated with acidic carboxylic groups and basic 3-aminopyridine moieties, creates a synergistic environment that facilitates the multi-component reaction. The acidic sites activate the carbonyl oxygen of the aldehyde, making it more susceptible to nucleophilic attack, while the basic sites simultaneously deprotonate the malononitrile. This cooperative activation lowers the energy barrier for the Knoevenagel condensation and subsequent Michael addition, allowing the reaction to proceed efficiently under mild, environmentally friendly conditions (EtOH/H2O, 50 °C). The successful recycling of the catalyst for several cycles with minimal loss of activity further demonstrates its stability and the strength of the covalent functionalization between the 3-aminopyridine and the GO support.

The biological findings of this study provide clear qualitative insight into the structure-activity relationship (SAR) of the synthesized chromenes. The results indicate that anticancer potency is not a generic property of the scaffold but depends strongly on the electronic and lipophilic nature of the substituents on the phenyl ring. A significant finding is the enhanced activity of compound 4b, which contains a bromine atom at the para position. From a medicinal chemistry perspective, introducing a halogen atom such as bromine increases the molecule's lipophilicity, a critical factor for effective passive transport across hydrophobic cancer cell membranes. This observation is in strong agreement with previous research indicating that halogenated benzopyrans often exhibit superior pharmacological profiles due to improved cellular uptake (3, 4, 33).

Furthermore, the selectivity observed between cancerous and normal cell lines (HFF) is among the most promising implications of this study. While the reference drug doxorubicin shows high potency, its relatively low selectivity index indicates a risk of significant off-target toxicity. In contrast, the synthesized dihydropyrano[3,2-c]chromenes, particularly the methoxy-substituted derivative 4d, demonstrated a remarkable safety

[Downloaded from ijpho.ssu.ac.ir on 2026-11-24]

[DOI: 10.18502/ijpho.v16i2.21344]

This article is distributed under the terms of the Creative Commons Attribution-NonCommercial 4.0 International License.

margin. The electron-donating methoxy group may modulate the interaction of the chromene core with specific intracellular targets overexpressed in cancer cells, such as those involved in apoptosis or cell cycle regulation, while remaining relatively inert in normal fibroblasts (34-37). Conversely, heterocyclic substitution in compounds 4g and 4h resulted in a varied response across cell lines, suggesting that replacing the phenyl ring with a pyridyl moiety alters the molecular geometry and electronic density, which may influence binding affinity towards potential biological receptors.

The overall results indicate that these functionalized chromenes exert cytotoxic effects in a cell-line-dependent manner, likely through the induction of programmed cell death or inhibition of enzymes essential for tumour progression (7). Achieving high anticancer activity while maintaining low toxicity towards healthy cells positions these compounds as viable candidates for further drug optimization. This study bridges the gap between green catalytic synthesis and drug discovery, providing a robust method to generate biologically active heterocycles that meet the dual requirements of synthetic efficiency and therapeutic selectivity (38). Thus, the integration of a GO-based nano-catalytic system not only enables a sustainable synthetic pathway but also produces chromene derivatives with significant potential for targeted cancer therapy, particularly those bearing halogenated aryl groups, which demonstrated the most promising balance of potency and safety.

Conclusion

In general, by using GO/3-aminopyridine as an effective and strong catalyst in this work, we synthesized various chromene derivatives. Due to the presence of nitrogen groups on the surface of graphene oxide and carboxylic acid groups in the structure of graphene oxide, this catalyst exhibited strong acid-base properties. FT-IR, FESEM, EDX and XRD analyses were used to confirm the structure of the catalyst. In this research, chromene derivatives were synthesised using this nanocatalyst with high efficiency under balanced and suitable conditions in line with green chemistry principles. In addition, GO/3-aminopyridine retained high catalytic performance over at least six consecutive cycles (90% → 87% yield) with negligible leaching and preserved structural features, further supporting the green and reusable nature of the protocol. Considering the use of a green and reusable catalytic system and the acceptable inhibitory effect of these derivatives against cancer cells, this method can be considered a suitable candidate for the synthesis of pharmaceutical compounds.

Availability of Data

All data is available in manuscript.

Ethical Considerations

This study was conducted in accordance with the ethical standards of the Declaration of Helsinki and approved by the Research Ethics Committee of Shahid Sadoughi University of Medical Sciences, Yazd, Iran (Ethics Code: IR.SSU.MEDICINE.REC.1394.542).

Acknowledgements

ChatGPT was used solely for initial English language editing and improvement of grammar and phrasing. No AI was involved in the generation of scientific content, data analysis, interpretation, or the final writing of the manuscript. All research design, results, and conclusions were prepared by the authors.

Authors' Contributions

In this study, HE designed the study and supervised synthesizing the compounds, prepaired and editted the manuscript. LAZ performed the synthesis of the nanostructures and their characterizations. HZZ managed the biological assessment and editted the manuscript, AAMH contributed to the synthesis of compounds, SKh contributed to the synthesis of nanostructures. BZM performed the biological experiments.

Funding

This study did not receive any specific funding.

[Downloaded from ijpho.ssu.ac.ir on 2026-11-24]

[DOI: 10.18502/ijpho.v16i2.21344]

This article is distributed under the terms of the Creative Commons Attribution-NonCommercial 4.0 International License.

Conflict of Interest

The authors declare that they have no conflicts of interest.

References

1. Dehkordi M F, Dehghan G, Mahdavi M, Hosseinpour Feizi M A. Multispectral studies of DNA binding, antioxidant and cytotoxic activities of a new pyranochromene derivative. Spectrochim Acta A Mol Biomol Spectrosc 2015; 145: 353-359.

2. Nguyen Ngoc Huyen T, Nguyen Ngoc Phuong U, An TN, Nguyen Thi Hong A. Synthesis of a novel coumarin via the Mannich reaction: in vitro and in silico evaluation of anti-cancer, antimicrobial and antioxidant activities. R Soc Open Sci 2025 Oct 1;12(10): 1-22.

3. El-Agrody AM, Fouda AM, Khattab ES. Halogenated 2-amino-4 H-benzo [h] chromene derivatives as antitumor agents and the relationship between lipophilicity and antitumor activity. Med Chem Res 2017; 26: 691-700.

4. El-Agrody AM, Abd-Rabboh HS, Al-Ghamdi AM. Synthesis, antitumor activity, and structure–activity relationship of some 4 H-pyrano [3, 2-h] quinoline and 7 H-pyrimido [4′, 5′: 6, 5] pyrano [3, 2-h] quinoline derivatives. Med Chem Res 2013; 22: 1339-1355.

5. Abrunhosa L, Costa M, Areias F, Venaˆncio A, Proenca F. Antifungal activity of a novel chromene dimer. J Ind Microbiol Biotechnol 2007; 34: 787-792.

6. Jahangard E, Khazdooz L, Zarei A. Synthesis and in vitro antibacterial study of dihydropyrano[3,2-c]chromene derivatives by nano fluoro apatite doped with Mg and Si as a cooperative catalyst. Iran. J Catal 2020; 10: 57-63.

7. Mohamed HM. A comprehensive review on chromene derivatives: potent anti-cancer drug development and therapeutic potential. Orient J Chem 2025; 41: 584- 608.

8. Heravi M, Jani A M, Derikvand F, Bamoharram F F, Oskooie H A. Three component, one-pot synthesis of dihydropyrano[3,2-c]chromene derivatives in the presence of H6P2W18O62•18H2O as a green and recyclable catalyst. Catal Commun 2008; 10: 272–275.

9. Wang H J, Lu J, Zhang Z H. Highly efficient three component, one-pot synthesis of dihydropyrano[3,2-c]chromene derivatives. Monatsh Chem 2010; 141: 1107–1112.

10. Mehrabi H, Kazemi-Mireki M. CuO nanoparticles: an efficientand recyclable nanocatalyst for the rapid and green synthesis of 3,4-dihydropyrano[c]chromenes. Chin Chem Lett 2011; 22: 1419–1422.

11. Mansoor S Sh., Logaiya K, Aswin K, Sudhan P N. An appropriate one-pot synthesis of 3,4-dihydropyrano[c]chromenes and 6-amino-5-cyano-4-aryl-2-methyl-4H-pyrans with thiourea dioxide as an efficient, reusable organic catalyst in aqueous medium. J Taibah Univ Sci 2015; 9: 213–226.

12. Vafajoo Z, Veisi S Sh., Maghsoodlou M T, Ahmadian H. Electrocatalytic multicomponent assembling of aldehydes, 4-hydroxycoumarin and malononitrile: An efficient approach to 2-amino-5-oxo-4,5-dihydropyrano(3,2-c) chromene-3-carbonitrile derivatives. C R Chimie 2014; 17: 301-304.

13. Wang Y, Zuo H Ye G, Luo J. Synthesis of a novel poly (ethylene glycol) grafted N, N-dimethylaminopyridine functionalized dicationic ionic liquid and its application in one-pot synthesis of 3,4-dihydropyrano[3,2-c]chromene derivatives in water. J Mol Liq 2015; 212: 418–422.

14. Azarifar D, Khaleghi-Abbasabadi M. 'Fe3O4-supported N-pyridine-4-amine-grafted grapheme oxide as efficient and magnetically separable novel nanocatalyst for green synthesis of 4H-chromenes and dihydropyrano[2,3-c] pyrazole derivatives in water. Res Chem Intermed 2019; 45: 199-202.

15. Mollashahi E, Nikraftar M. Nano-SiO2 catalyzed three-component preparations of pyrano[2,3-d] pyrimidines, 4H-chromenes, and dihydropyrano[3,2-c]chromenes. J Saudi Chem Soc 2018; 22: 42-48.

16. Ghashang M, Mansoor S S, Shams Solaree L, Sharifian-esfahani A. Multi-component, one-pot, aqueous media preparation of dihydropyrano [3,2-c] chromene derivatives

[Downloaded from ijpho.ssu.ac.ir on 2026-11-24]

[DOI: 10.18502/ijpho.v16i2.21344]

This article is distributed under the terms of the Creative Commons Attribution-NonCommercial 4.0 International License.

over MgO nanoplates as an efficient catalyst. Iran J Catal 2016; 6: 237–243.

17. Maleki B. Green Synthesis of bis-Coumarin and Dihydropyrano[3,2-c]chromene Derivatives Catalyzed by o-Benzenedisulfonimide, Org Prep Proced Int 2016; 48: 303–318.

18. Asadpour Behzadi S, Sheikhhosseini E, Ahmadi S A, Ghazanfari D, Akhgar M, mefenamic acid as environmentally catalyst for three-component synthesis of dihydropyrano [2,3-c]chromene and pyrano[2,3-d]pyrimidine derivatives. J Applied Chemical Res 2020; 14: 63-73.

19. Wang Ch, Karmakar B, Awwad N S, Ibrahium H A, El-kott A F, Abdel-Daim M M, et al. Bio-supported of Cu nanoparticles on the surface of Fe3O4 magnetic nanoparticles mediated by Hibiscus sabdariffa extract: Evaluation of its catalytic activity for synthesis of pyrano[3,2-c] chromenes and study of its anti-colon cancer properties. Arab J Chem 2022; 15: 1-14.

20. Sheikhhosseini E, Yahyazadehfar M, Synthesis and characterization of an Fe-MOF@Fe3O4 nanocatalyst and its application as an organic nanocatalyst for one-pot synthesis of dihydropyrano[2,3-c]chromenes. Front Chem 2022; 10: 1-12.

21. Palapetta S Ch, Gurusamy H, Ganapasam S. Synthesis, Characterization, Computational Studies, Molecular Docking, and In Vitro Anticancer Activity of Dihydropyrano[3,2-c]chromene and 2-Aminobenzochromene Derivatives. ACS Omega 2023; 8: 7415-7429.

22. Teo P S, Lim H N, Huang N M, Chia C H, Harrison I. Room temperature in situ chemical synthesis of Fe3O4/Graphene. Ceram Int 2012; 38: 6411-6416.

23. Yang X, Zhang X, Ma Y, Huang Y, Wang Y, Chen Y. Superparamagnetic graphene oxide-Fe3O4nanoparticles hybrid for controlled targeted drug carriers. J Mater Chem 2009; 19: 2710-2714.

24. Orie K, Duru R, Ngochindo R. Synthesis, complexation and biological activity of aminopyridine: a mini-review. Am j Heterocycl Chem 2021; 7: 11–25.

25. Khabnadideh S, Khorshidi Kh, Amiri-Zirtol L. A novel heterogeneous acid–base nano-catalyst designed based on graphene oxide for synthesis of spiro-indoline-pyranochromene derivatives. BMC Chem 2023; 17: 1-13.

26. Mallakpour S, Abdolmaleki A, Borandeh S. Covalently functionalized graphene sheets with biocompatible natural amino acids. Appl Surf Sci 2014; 307: 533–542.

27. Undeger U, Başaran A, Degen G H, Başaran N. Antioxidant activities of major thyme ingredients and lack of (oxidative) DNA damage in V79 Chinese hamster lung fibroblast cells at low levels of Carvacrol and Thymol. J Food Chem Toxicol 2009; 47: 2037-2043.

28. Jahangard E, Khazdooz L, Zarei A. Synthesis and in vitro antibacterial study of dihydropyrano [3, 2-c] chromene derivatives by nano fluoro apatite doped with Mg and Si as a cooperative catalyst. Iran J Catal 2020; 10: 57-63.

29. Baziar A, Ghashang M. Preparation of Pyrano[3,2-c] Chromene-3-Carbonitriles using ZnO nano-particles: A comparison between the box–behnken experimental design and traditional optimization methods. React Kinet Mech Catal 2016; 118: 463–479.

30. Mehrabi H, Abusaidi H. ynthesis of Biscoumarin and 3,4-Dihydropyrano[c]chromene Derivatives Catalysed by Sodium Dodecyl Sulfate (SDS) in Neat Water. J Iran Chem Soc 2010; 7: 890-894.

31. Mirjalilia B B F, Mehravar M, Bamoniri A, Babaei E. Three-component, one-pot synthesis of Dihydropyrano[3,2-c]chromenes in aqueous medium in the presence of nano-silica supported 1,5-Diazabicyclo(4.3.0)non-5-en. Org Chem Res 2021; 7: 127-138.

32. Montazer N, Antibacterial activity and efficient synthesis of 3,4 dihydropyrano [c] chromene

derivatives by using ammonium trifluoroacetate (CF3COONH4) catalyst. Iran J Med Microbiol 2017; 11: 61-68.

33. Shafiee A, Motamedi R, Firuzi O, Meili S, Mehdipour A R, Miri R. Synthesis and syttotoxic activity of novel benzopyrano[3,2 –c]chromene-6,8-dione derivatives. Med Chem

[Downloaded from ijpho.ssu.ac.ir on 2026-11-24]

[DOI: 10.18502/ijpho.v16i2.21344]

This article is distributed under the terms of the Creative Commons Attribution-NonCommercial 4.0 International License.

Res 2011; 20: 466–474.

34. Braga T C, Silva M M, Nascimento E O O, Silva E C D, Rego Y F, Mandal M, et al. Synthesis, anticancer activities and experimental-theoretical DNA interaction studies of 2-amino-4-phenyl-4H-benzo[h]chromene-3-carbonitrile'. European J Med Chem Reports 2022; 4: 1-12.

35. Esmati N, Foroughian M, Saeedi M, Mahdavi M, Khoshneviszadeh M, Firuzi O R.N, et al. Synthesis and cytotoxic activity of some novel Dihyrobenzo[h]pyrano [3,2-c]chromene derivatives. J Heterocyclic Chem 2015; 52: 97.

36. Afifi TH, Okasha RM, Alsherif H, Ahmed HE, Abd-El-Aziz AS. Design, synthesis, and docking studies of 4H-chromene and chromene based azo chromophores: a novel series of potent antimicrobial and anticancer agents. Curr Org Synth 2017; 14: 1036–1055.

37. Ahmed HEA, El-Nassag MAA, Hassan AH, Okasha RM, Ihmaid S, Fouda AM, et al. Introducing novel potent anticancer agents of 1H benzo[f]chromene scaffolds, targeting c-Src kinase enzyme with MDA-MB-231 cell line anti-invasion effect. J Enzyme Inhib Med Chem 2018; 33: 1074–1088.

38. Abaszadeh M, Ebrahimi A, Sabouri S. Investigating the in vitro antiproliferative and apoptosis inducing effects of pyranochromene derivatives. Biointerface Res Appl Chem 2021; 11: 10987 -10995.

[Downloaded from ijpho.ssu.ac.ir on 2026-11-24]

[DOI: 10.18502/ijpho.v16i2.21344]

This article is distributed under the terms of the Creative Commons Attribution-NonCommercial 4.0 International License.